

Quantitative ^2H NMR spectroscopy

1. Thermodynamic H/D isotope effects in *N,N*-dimethylformamide and cyclopentadiene molecules

V. A. Roznyatovsky, S. M. Gerdov, Yu. K. Grishin,* D. N. Laikov, and Yu. A. Ustynyuk

Department of Chemistry, M. V. Lomonosov Moscow State University,
Leninskie Gory, 119992 Moscow, Russian Federation.
Fax: +7 (095) 939 2677. E-mail: ygri@nmr.chem.msu.su

A new method for quantification of the relative distribution of deuterium in molecules is proposed. The technique is based on the lineshape analysis in the ^2H NMR spectra obtained at the natural abundance level of deuterium with allowance for inhomogeneity of the magnetic field. The equilibrium thermodynamic H/D isotope effects for hindered rotation about the C–N bond in the *N,N*-dimethylformamide molecule and for prototropic exchange in the cyclopentadiene molecule were determined. The results obtained agree with those of DFT calculations of the vibrational energies.

Key words: thermodynamic H/D isotope effect, deuterium, ^2H NMR spectroscopy, *N,N*-dimethylformamide, cyclopentadiene.

Relatively large mass difference between protium and deuterium (two stable isotopes of hydrogen) causes pronounced and readily detectable H/D isotope effects in physicochemical processes. This has been widely used in studies of reaction mechanisms.¹ Marked inhomogeneity of the distribution of deuterium in organic molecules and large deviations of the content of deuterium from the averaged natural abundance (155.8 ppm)² are determined by the kinetic isotope effect, which is due to different reaction rates of isotopomers, and by the thermodynamic isotope effect resulting from different rovibrational energies of the isotopomers. Selective distribution of biogenic compounds reflects their prehistory and can be used in studies of biosynthetic pathways and for the determination of a natural source from which a particular compound was isolated.³

Isotope mass spectrometry is most widely and successfully used for the determination of overall isotope composition of organic compounds. However, this technique is of little use for studying the selectivity of isotope distribution over structural positions in molecules and requires a stepwise chemical decomposition of the molecules prior to the mass spectrometry experiments.³ In this respect unquestionable advantages are provided by NMR spectroscopy. Both stable isotopes of hydrogen have the magnetic moments (Table 1) and can therefore be studied by NMR spectroscopy. However, acquisition of

Table 1. Properties of stable isotopes of hydrogen

Isotope	Spin	<i>C</i> (%)	<i>I</i>	<i>I</i> _{rel}
^1H	1/2	99.984	1.00	1.00
^2H	1	0.016	$9.65 \cdot 10^{-3}$	$1.45 \cdot 10^{-6}$

Note. *C* is the natural abundance of the isotope, *I* is the relative sensitivity, and *I*_{rel} is the relative sensitivity with allowance for the natural abundance of the isotope.

the ^2H NMR spectra at the natural abundance level presents some difficulties. Because of the low natural abundance of deuterium and the smaller magnetic moment of deuteron the intensity of signals in the ^2H NMR spectra is as little as $1.45 \cdot 10^{-6}$ of the signal intensity in the ^1H NMR spectra.

In this connection, obtaining a needed signal-to-noise ratio requires long-term signal accumulation or experiments with isotopically enriched samples. In particular, information on the influence of the primary and secondary H/D isotope effects on the chemical shifts and spin–spin coupling constants in organic molecules was for the most part obtained using deuterated compounds.⁴ Deuterium has a quadrupole moment ($2.77 \cdot 10^{-28}$ m²); however, relatively long spin-lattice relaxation times, *T*₁, of the ^2H nuclei in organic molecules (0.1–7 s) allow one to obtain rather narrow spectral lines in solutions. The quadrupole mechanism contributes predominantly to the nuclear relaxation of deuterium. Therefore, no Overhauser effect is observed when recording the proton decoupling

* Dedicated to Academician I. P. Beletskaya on the occasion of her anniversary.

spectra and the signal intensities remain undistorted, thus favoring quantification experiments.³

The ²H NMR spectroscopy at the natural abundance level offers considerable advantages despite relatively weak signals. First, there is no need in the synthesis of selectively deuterated or perdeuterated compounds. Then, the ²H NMR spectra represent superpositions of the spectra of isotopomers containing a single deuterium atom in each molecule because of the low natural abundance of deuterium. Finally, all signals in the proton decoupling spectra are singlets while their integrated intensities exactly correspond to the content of deuterium in each inequivalent structural position, thus providing direct information on the selective isotope distribution in the molecule.

Differences in signal intensities due to the isotope effects in the ²H NMR spectra obtained at the natural abundance level of deuterium are often small (sometimes, they are as little as fractions of a per cent). Their determination requires high accuracy of integration of the resonance signals. Standard procedures for numerical integration of the NMR spectra exhibiting no too overlapped lines provide an accuracy of about 1–2%, which is sufficient for solving most of routine tasks if a necessary signal-to-noise ratio is achieved. Earlier,⁵ it was also proposed to use the peak intensities of ²H NMR signals for solving some specific problems. However, this can lead to rather large systematic errors due to the fact that the relaxation times of the ²H nuclei occupying different positions in the molecule differ appreciably and, hence, the corresponding resonance signals have different widths.⁶ Because of this, highly accurate integration of NMR signals is often performed using a conventional spectral deconvolution procedure. In this case, the total spectral contour is approximated by a superposition of Lorentzian lines and the best agreement between the experimental and calculated spectra is achieved by varying the positions, widths, and intensities of spectral lines. This approach is highly efficient when all lines are sufficiently well resolved singlets and the exact number of lines is known.⁷ Standard subroutines for spectral deconvolution are incorporated into software packages supplied with commercially available NMR spectrometers (see, e.g., Ref. 8). Given a high signal-to-noise ratio and a representative sample volume (number of experiments), statistical processing of the results obtained for small molecules can provide the values 0.2–0.3% for the accuracy of measurements using the integrated intensities.⁹ Further improvement of the accuracy requires taking account of the deviations of the shape of real lines in the absorption spectrum from Lorentzian shape. These deviations are mainly due to residual inhomogeneity of the magnetic field and to the phase shift, provided a correct choice of experimental conditions and parameters for recording the

spectra. In the time domain this causes a non-exponential free induction decay (FID). An unconventional procedure⁶ for eliminating this effect involves representation of the experimental FID as a product of a Lorentzian function and a non-Lorentzian function. The necessary parameters of the non-Lorentzian weighting function can be found from the FID of a reference sample assuming that measurements using different samples are carried out under the same experimental conditions. The last-named requirement is very rigorous and cannot be met in real high-resolution experiments.

To study the selectivity of the distribution of deuterium in organic molecules at the natural abundance level of this isotope, in this work we developed a more convenient iterative procedure for calculating the total lineshape of resonance absorption with direct allowance for phase distortions and residual inhomogeneity of the polarizing magnetic field. The accuracy of determination of the integrated intensities of spectral lines is high enough to open up new prospects for quantification of the thermodynamic and kinetic H/D isotope effects in organic molecules of not too high molecular weights (up to 300–400 Da). In this work we measured the thermodynamic H/D isotope effects for *N,N*-dimethylformamide (DMF) and cyclopentadiene. Comparison of the experimental data and the results of calculations using high-level methods of quantum chemistry revealed good qualitative agreement.

Experimental

N,N-Dimethylformamide (Merck) was used as-received. Cyclopentadiene was distilled immediately prior to the experiments from a cyclopentadiene–cyclopentadiene dimer mixture (25 °C, $1 \cdot 10^{-2}$ Torr).

¹H (300.13 MHz) and ²H (46.05 MHz) NMR spectra were recorded on a Bruker DPX-300 spectrometer equipped with a 10-mm deuterium selective probe. Stabilization of the resonance conditions was achieved using the ¹⁹F signal. The duration of the 90° pulse for the ²H nuclei was 18 μs. The WALTZ-16 pulse sequence was employed for broadband proton decoupling. In the case of DMF measurements were carried out using an ampule (o.d. 10 mm) and a coaxial cylindrical capillary (2 mm in diameter) filled with hexafluorobenzene and placed inside the ampule. In the experiments with cyclopentadiene hexafluorobenzene (5 vol.%) was added immediately to the sample. The spin-lattice relaxation times of deuterium nuclei, T_1 , were measured using the method of inversion–recovery of the nuclear magnetization vector. The relaxation delay between repetitions of the pulse sequence during the accumulation of ²H NMR signals was at least $5T_1$. The acquisition time, AQ, of the free induction decay signal was at least $4T_1$ (12 s for DMF and 6 s for cyclopentadiene). The number of scans was chosen in such a way as to achieve an optimum signal-to-noise ratio. The overall duration of the experiments on acquiring the ²H NMR spectra was 12 h for DMF and 4h for cyclopentadiene.

Results and Discussion

Total lineshape analysis of NMR spectra with allowance for residual inhomogeneity of the magnetic field.

The INTSPECT2 iterative program

In the absence of exchange processes the line contours in the NMR spectra of liquids differ from the ideal Lorentzian shape mainly due to inhomogeneity of the magnetic field within the sample. This is most pronounced in the case of signals with small natural width determined by relaxation processes. By correcting non-ideal magnet design using shim coils one can reduce inhomogeneity of the magnetic field to nearly 10^{-9} , which allows line narrowing down to 0.1 Hz. However, correction of distortions introduced by the probe coil and by the sample in the regions characterized by abrupt changes in the magnetic susceptibility (*e.g.*, at glass–solution boundaries) using shim coils is virtually unfeasible. This type of distortions causes line broadening at the base. Inhomogeneous line broadening can also be due to instability of the resonance conditions with time due to field drift, low sensitivity, or noise in the stabilization channel. In this case the spectrum is a superposition of signals obtained from each voxel of the sample during each scan and spectral information on the spatial and temporal inhomogeneity of the magnetic field is averaged. Because of this, reconstruction of actual three-dimensional field distribution within the sample is impossible.

The height (H) and halfwidth ($\Delta\nu_{1/2}$) of a Lorentzian spectral line unambiguously determine the area under the curve ($S = \pi H \Delta\nu_{1/2} / 2$). This permits calculations of the integrated intensities of signals using deconvolution techniques in the absence of inhomogeneous line broadening. Convolution of the Lorentzian line with a line of unit area does not change the area under the curve. This allows one to construct a special function determined by inhomogeneity of the magnetic field within the sample and then to convolve it with the Lorentzian line to reproduce the experimental shape of the signal.

Similarly to other deconvolution programs, the INTSPECT2 program is based on nonlinear regres-

sion analysis.¹⁰ All spectral lines are approximated by Lorentzian lines. Theoretical spectrum is calculated using convolution with a normalized function obtained from the dependence of the magnetic field strength along the Z axis. The phase shift is achieved by mixing the dispersion and absorption signals.

To simulate the residual inhomogeneity of the magnetic field, we chose the orthogonal gradients Z^1 – Z^8 directed along the axis of the sample. The contributions of the XZ , YZ , and higher gradients to the total inhomogeneity of the magnetic field does not differ from the contributions of longitudinal gradients Z^1 – Z^8 , since the field inhomogeneity due to the X and Y gradients can be efficiently averaged by rotating the sample. This allowed the magnetic field to be treated as both spatially (in the XY plane) and temporally homogeneous. The choice of gradients up to the eight order permitted simulation of drastic changes the magnetic field strength within the sample.

By varying the parameters of the iterative procedure (position, height, and halfwidth of each line, base line (bias) level, zero- and first-order phases, and the Z^1 – Z^8 gradients) one can achieve best agreement between the simulated and experimental spectra.

The program was tested taking integration of signals of a sample containing a mixture of chloroform, methylene chloride, 1,2-dichloroethane (DCE), tetramethylurea (TMU), acetone, and cyclohexane as an example (all individual compounds exhibit singlet ^1H NMR spectra). Three types of the ^1H NMR spectra of this mixture of solvents were processed by the program. The experimental conditions for recording the spectra were as follows: (a) optimum shimming of the magnetic field and phase-matching, (b) as in the case *a* followed by distortion of the Z^3 and Z^4 gradients, and (c) as in the case *a* with addition of zero- and first-order phase distortions. The integrated intensities, S , of the lines in these spectra calculated using the INTSPECT2 program and normalized to the intensity of the signal of cyclohexane are listed in Table 2. The results obtained indicate that the program provides a good convergence under different experimental conditions.

We found that the above-mentioned procedure permits higher accuracy of calculations compared to conventional integration techniques. Unquestionable advan-

Table 2. Results of integration of the ^1H NMR spectra recorded under different conditions (*a*–*c*). The integrated intensities, S , were normalized to the intensity of the signal of cyclohexane

Solvent	$S(a)$	$S(b)$	$S(a) - S(b)$	$S(c)$	$S(b) - S(c)$
CHCl_3	1.196 ± 0.002	1.193 ± 0.002	0.003 ± 0.004	1.195 ± 0.002	0.001 ± 0.004
CH_2Cl_2	1.317 ± 0.002	1.319 ± 0.002	0.002 ± 0.004	1.315 ± 0.002	0.002 ± 0.004
DCE	0.897 ± 0.002	0.899 ± 0.002	0.002 ± 0.004	0.895 ± 0.002	0.002 ± 0.004
TMU	1.369 ± 0.002	1.373 ± 0.002	0.004 ± 0.004	1.367 ± 0.002	0.002 ± 0.004
Me_2CO	1.967 ± 0.002	1.969 ± 0.002	0.002 ± 0.004	1.964 ± 0.002	0.002 ± 0.004
<i>cyclo</i> - C_6H_{12}	1.000	1.000	—	1.000	—

tages of our program manifest themselves when analyzing overlapped signals. In this case the quantification technique using the intensities of spectral lines is inapplicable.

Isotope distribution of deuterium in DMF molecule

Thermodynamic (equilibrium) H/D isotope effects in systems with intramolecular exchange processes have been studied by a number of experimental methods taking various isotopically enriched compounds as examples.^{3,11–13} The equilibrium isotope effects can serve as a measure of difference between the local force fields at two different positions which can be occupied by a particular isotope. To the best of our knowledge, the heavy isotope always predominantly occupies the most sterically hindered position. Qualitatively, this can be explained by the fact that the equilibrium C–D bond lengths are always about $5 \cdot 10^{-3}$ Å smaller than the C–H bond lengths.^{14,15} In this connection deuterium-containing groups are somewhat smaller than protium-containing ones.

Internal rotation about the C–N bond in carboxylic acid amide molecules is hindered due to some degree of double bonding in this bond. This process in DMF has been repeatedly studied.¹⁶ For neat liquid DMF the activation barrier, ΔG_{298}^\ddagger , is 21.8 kcal mol⁻¹.¹⁷ This means that at room temperature the dynamic exchange process is very slow in the NMR time scale and contributes negligibly to the linewidth ($\leq 10^{-3}$ Hz). At the same time the equilibrium (1) between the *cis*-DMF and *trans*-DMF isotopomers containing a deuterium atom in one Me group should be established rapidly ($\sim 10^3$ s) and readily under the experimental conditions.

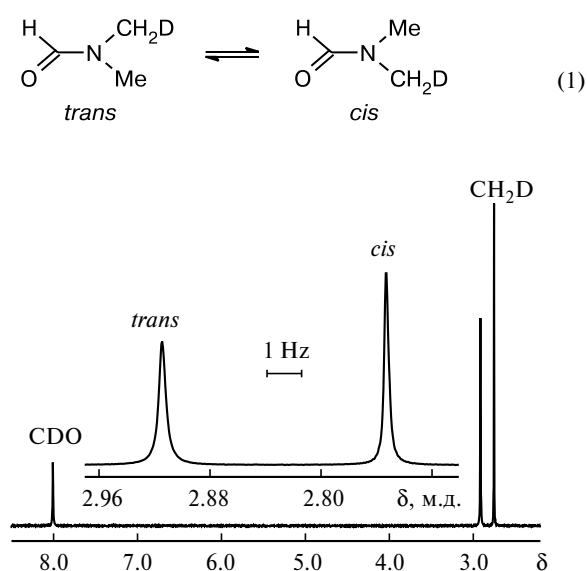


Fig. 1. ²H NMR spectrum of DMF (46.05 MHz) at 303 K.

Table 3. Relaxation times (T_1/s), relative integrated intensities* (S), and linewidths ($\Delta\nu_{1/2}/\text{Hz}$) in the ²H NMR spectrum of DMF at 303 K

Group	T_1/s	S	$\Delta\nu_{1/2}$
<i>trans</i> -CH ₂ D	1.5	1.023(3)	0.24
<i>cis</i> -CH ₂ D	3.4	1.000(3)	0.13
CDO	1.2	1.254(16)	0.35

* Calculated per hydrogen atom.

The ²H NMR of pure DMF is shown in Fig. 1. The signals of the Me groups at the nitrogen atom were assigned based on the results of ¹H NMR DIFNOE experiment with irradiation of the formyl proton signal. In the 7 T field the ²H resonance frequency difference between different isotopomers is rather large and at 303 K two Me groups exhibit well-resolved narrow singlets with the linewidths determined by corresponding relaxation times.

The longitudinal relaxation times, T_1 , of deuterium nuclei in DMF are listed in Table 3. The T_1 values of the Me groups in *cis*- and *trans*-positions with respect to the oxygen atom are appreciably different due to anisotropy of molecular rotation.¹⁸ Relaxation processes in DMF are responsible for marked differences in widths and, hence, peak intensities of the spectral lines. In this case evaluation of the integrated intensities S requires the use of total lineshape analysis.

Analysis of the data listed in Table 3 shows that the difference between the integrated intensities S of the lines of DMF isotopomers is significantly larger than the measurement error. Thermodynamically more favorable are those isotopomers in which the CH₂D group is in *trans*-position relative to the oxygen atom. Noteworthy is that the formyl group in DMF is deuterium enriched (calculated per hydrogen atom) compared to the Me groups. The ratio of the integrated intensities of the signals of Me groups is equal to the constant of equilibrium (1).

The results of our measurements of thermodynamic isotope effect in DMF are in good agreement with the results of high-level quantum-chemical calculations.*

Selective distribution of deuterium in cyclopentadiene molecule

A feature of cyclopentadiene molecule is a degenerate prototropic rearrangement by the mechanism of 1,5-sigmatropic shift with an activation energy of ~ 25 kcal mol⁻¹.^{19,20} Introduction of the deuterium label into the cyclopentadiene molecule removes the degen-

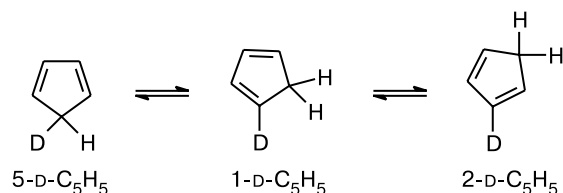
* O. V. Yazev and Yu. A. Ustynyuk. Unpublished results.

Table 4. ^2H NMR spectral parameters and calculated rovibrational energies (E) of cyclopentadiene isotopomers

Molecule	T_1/s	S^*	$E/\text{kcal mol}^{-1}$	
			harm.	anharm.
1-D-C ₅ H ₅	1.4	0.992(3)	54.269	54.575
2-D-C ₅ H ₅	1.5	1.020(3)	54.247	54.486
5-D-C ₅ H ₅	1.5	0.988(3)	54.293	54.509

* Integrals were normalized to the average value.

eracy and the dynamic process leads to establishment of equilibrium between three isotopomers:



The prototropic rearrangement occurs at rather high rates at the temperatures required for the synthesis of cyclopentadiene from its dimer following the retro-Diels–Alder reaction ($>140\text{ }^\circ\text{C}$). The deuterotropic rearrangement (degenerate exchange in the case of mono-deuterocyclopentadiene) is characterized by a much higher energy barrier ($>33\text{ kcal mol}^{-1}$).¹⁹ At ambient temperatures the ^2H NMR spectrum of cyclopentadiene corresponds to stereochemically rigid state of the molecule; the 1-D-, 2-D-, and 5-D-isotopomers exhibit narrow signals at δ 6.15, 6.21, and 2.81, respectively. Spectral measurements for quantitative integration were carried out using a freshly prepared sample at $-10\text{ }^\circ\text{C}$ (in this case the dimerization according to Diels–Alder is strongly hindered). The duration of the experiments was limited to four hours to avoid the appearance of the signals of cyclopentadiene dimer. Relatively fast deuterium nuclear relaxation in this compound provided a rather high signal-to-noise ratio (180) in the course of the experiments. The parameters of the ^2H NMR spectra of cyclopentadiene are listed in Table 4. The integrated intensities of spectral lines were normalized to the average value.

The population differences between the three isotopomers exceed the measurement error. The 5-D-isomer containing the deuterium atom in the methylene group was found to be least stable. The molecules in which the heavy isotope of hydrogen is located at the double bond are characterized by a rather large population difference (over 2%).

Table 4 also lists the rovibrational energies of three isotopomers of cyclopentadiene calculated both in the

harmonic and anharmonic approximation using the DFT approach with the PBE functional and the TZ2p basis set (the PRIRODA program).²¹ The experimental data are in good agreement with the results of quantum-chemical calculations in the harmonic approximation. Calculations in the anharmonic approximations correspond to the spectral data for the unsaturated molecular fragment and predict the highest stability for the 2-D-C₅H₅ molecule.

This work was carried out with the financial support of the Russian Foundation for Basic Research (Project Nos. 02-03-33030).

References

1. L. Melander and W. H. Saunders, *Reaction Rates of Isotopic Molecules*, Wiley, New York, 1980, 340 pp.
2. R. Hagemann, G. Nief, and E. Roth, *Tellus*, 1970, **22**, 712.
3. M. L. Martin and G. J. Martin, *NMR Basic Principl. Progr.*, 1990, **23**, 3.
4. H. H. Mantsch, H. Saito, and I. C. P. Smith, *Prog. Nucl. Magn. Reson. Spectrosc.*, 1977, **11**, 211.
5. G. J. Martin, X. Y. Sun, C. Guillou, and M. L. Martin, *Tetrahedron*, 1985, **41**, 3285.
6. M. A. Cremonini, D. Tacconi, V. Clementi, and C. Luchinat, *J. Agric. Food Chem.*, 1998, **46**, 3943.
7. T. Nakayama and Y. Fujlwar, *Anal. Chem.*, 1982, **4**, 25.
8. Xwin-nmr Software Manual. Part 1: General Features and Data Processing, Bruker Analytik GmbH, 1997, 185.
9. G. J. Martin and N. Naulet, *Fresenius' Z. Anal. Chem.*, 1988, **332**, 648.
10. K. Ebert and H. Ederer, *Computeranwendungen in der Chemie*, Verlagsgesellschaft mbH, Weinheim, 1985, 370 pp.
11. U. Siehl, *Adv. Phys. Org. Chem.*, 1987, **23**, 63.
12. P. E. Hansen, *Prog. Nucl. Magn. Reson. Spectrosc.*, 1988, **20**, 207.
13. B. L. Zhang, F. Marbon, and M. L. Martin, *J. Phys. Org. Chem.*, 1993, **6**, 367.
14. E. A. Halevi, *Prog. Phys. Org. Chem.*, 1963, **1**, 109.
15. C. Jameson and H. Osten, *J. Chem. Phys.*, 1984, **81**, 4293.
16. M. Oki, *Applications of Dynamic NMR spectroscopy to Organic Chemistry in Methods in Stereochemical Analysis*, VCH, 1985, 423.
17. R. C. Neumann, Jr. and V. Jonas, *J. Org. Chem.*, 1974, **39**, 925.
18. H. H. Mantsch, H. Saito, L. C. Leitch, and I. C. P. Smith, *J. Am. Chem. Soc.*, 1974, **96**, 256.
19. W. R. Roth, *Tetrahedron Lett.*, 1964, 1009.
20. N. M. Sergeev, *Prog. Nucl. Magn. Reson. Spectros.*, 1975, **9**, 71.
21. D. N. Laikov, Ph.D. Thesis, M. V. Lomonosov Moscow State University, Moscow, 2000 (in Russian).

Received October 8, 2002;
in revised form December 4, 2002